DETECTION OF RISKY MOUNTAIN STREAM AND SLOPE FAILURE AREA IN NORO-GAWA RIVER BASIN USING GIS AND OPTICAL SATELLITE IMAGE

KOJI ASAI
Yamaguchi University, Ube, Japan, kido@yamaguchi-u.ac.jp

TOMOHIRO ISHII
Yamaguchi University, Ube, Japan, i006ve@yamaguchi-u.ac.jp

TAKUZO AMANO
Chuden Engineering Consultants, Hiroshima, amano@cecnet.co.jp

HAJIME SHIROZU
Yamaguchi University, Ube, Japan, shiro@yamagichi-u.ac.jp

ABSTRACT

Several landslide disasters occurred in Hiroshima due to heavy rainfall of July 2018, and sediment and driftwood caused channel blockage and increased flood damages. Therefore, in order to consider the prevention and mitigation of heavy rain disasters, it is important to consider the effect of the flow into the sediment, driftwood of the river channel. In this study, taking the upstream of Norogawa dam as an example site, various investigations were carried out on slope failures that caused channel blockage. The slope failure region was extracted by optical satellite image, and the correspondence with the dangerous mountain stream with the possibility of the slope failure was evaluated by the least-cost analysis based on the slope of the ground. It was successfully detected the slope failures by using the satellite images before and after disaster. The improvement for the least-cost path analysis is required. However, it is found that this analysis would be useful for the qualitative usage.

Keywords: slope failure, GIS, remote sensing, heavy rain, optical satellite image

1. INTRODUCTION

Recently, heavy rainfall disasters become severe more and more in Japan. It would be anticipated that theses heavy rainfall disasters are induced by the climate change due to the global warming. The heavy rainfall occurred in west part of Japan in July 2018. This heavy rainfall induced flooding and landslides in very wide area. The slope failure occurred in the mountain area of which the geology is granite in Hiroshima Prefecture. The Norogawa River and Norogawa dam located in Yasuura Town, Hiroshima prefecture shown in Figure 1 were also damaged by this heavy rain disaster. The sediments and the driftwoods were deposited in the river channel and Norogawa dam in the upstream region of the Norogawa River. The deposition of them made the water level of Norogawa dam rise drastically, and then the wrong operation of the discharge from the dam were made. It is very important that the effect of sediments and driftwoods are considered when the measures for reducing metrological natural disasters is discussed.

Now a days, the methods for detecting a place of a slope failure with a satellite remote sensing are proposed (Eguchi and Miura (2016), Hayashi et. Al. (2012)). In this study, we have tried to detect the risky mountain streams and the slope failure areas using the satellite optical images and GIS for the rainfall disaster occurred in July 2018. Especially, the Norogawa River basin was focused on in this study. Firstly, we have conducted the extraction of the slope failure areas in the Norogawa River basin using the optical satellite images before and after the disaster occurred, and we have made a comparison of the accuracy of the extraction with the DEM (Digital Elevation Model) data. Secondary, we have conducted the least-cost path analysis with GIS to make a judgment that the sediments produced at a slope failure can reach the Norogawa River.

2. EXTRACTION OF SLOPE FAILURE AREA USING SATELLITE OPTICAL IMAGE

The optical satellite image before the disaster shotten (**Shorten?**)by WorldView-2 on 27 October 2017 and that after the disaster shotten by WorldView-3 on 15 July 2018 were used. The shooting condition of the optical images is shown in Table 1. The NDVI (Normalized Difference Vegetation Index) analysis and GSI (Grain Size Index) analysis were conducted to extract the slope failure areas.

NDVI is an index to indicate an activity of live green vegetations and is estimated with Eq. (1). GSI is an index to indicate a condition of the ground surface and is estimate with Eq. (2).

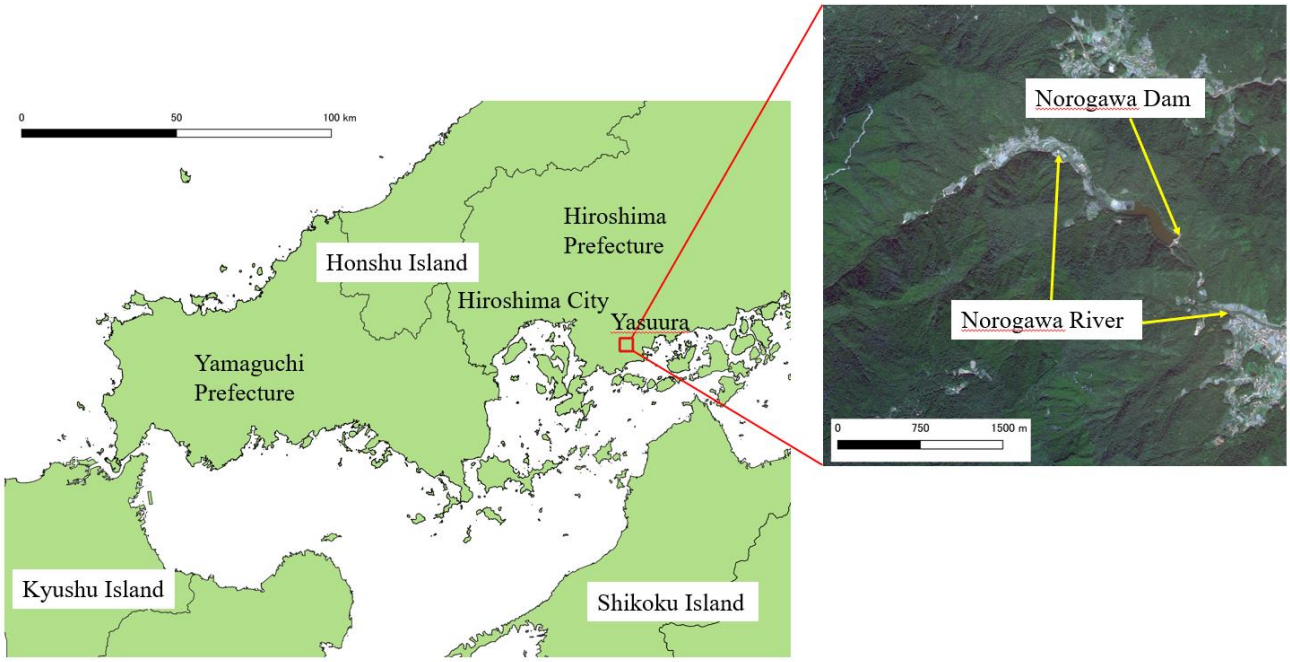

Figure 1. Location of Norogawa Dam and Norogawa River

Table 1. Shooting condition of optical satellite images

	Date	Satellite	Sensor	Resolution	Off nadir angle
Before disaster	27 Oct. 2017	World View-3	Panchromatic Radar	0.5(m)	22(degree)
After disaster	15 July 2018	World View-2	Panchromatic Radar	0.5(m)	37(degree)

$$\mathrm{NDVI} = \frac{IR - R}{IR + R} \tag{1}$$

$$\mathrm{GSI} = \frac{R - B}{R + G + B} \tag{2}$$

Where *IR* is the near infrared band, *R* is the visible red band, *B* is the visible blue band and *G* is the visible green band. NDVI takes the range from -1 to 1. It is indicated that the larger NDVI is the higher the activity of the vegetation is. GDI also takes the range from -1 to 1. It is indicated that the ground condition is a bare filed when GSI is larger.

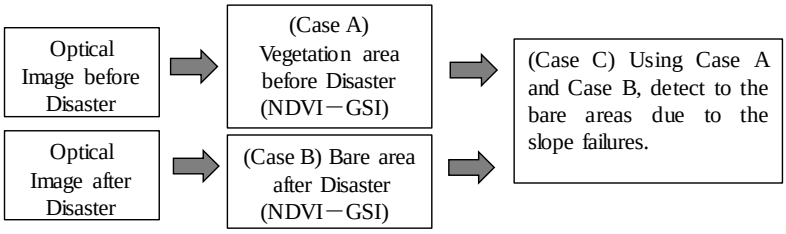

Figure 2. Analytical flow chart using NDVI and GSI

The NDVI image and the GSI image were created with the optical images before and after the disaster, and then the slope failure areas were extracted using the deference between the NDVI image and the GSI image. Figure 2 shows the analytical flow chart using NDVI and GSI. Figure 3 shows the extraction result of the slope failures with Cases A, B and C shown in Figure 2. The red lines indicate the slope failures or the marks of the debris flow. Figure 3(a) is the result obtained with the satellite images after the disaster (Case B). Comparing of Figure 3(a) to Fig.5 lately shown, we can see that the slope failures are extracted. However, the roads and houses are also extracted as the bare fields.

Figure 3(b) shows the result of Case C. This result was obtained with before and after the disaster. The slope failures can be extracted without roads and houses because of the uses of the image before the disaster. Figure 4 shows the slope failures in the mountain stream from the upstream side of Norogawa dam obtained by the Laser Profiler survey. The areas of the bear field due to the slope failures were evaluated for the satellite images and the Laser Profiler survey.

The areas evaluated with the satellite images and the Laser Profiler survey are 18.6 x 10^4 m^2 and 30.6 x 10^4 m^2, respectively. The area evaluated with the satellite images is smaller than that evaluated with the Laser Profiler survey. Comparing with Figure 3(b) and Figure 4 the slope failures on the left bank side of Norogawa River are extracted. On the other hand, the slope failures on the right bank side are not extracted well. This is why there is a discrepancy between the both slope failure areas. It would be considered for the low extraction of right bank side that the resolution of the optical satellite images is coarse more than the Laser Profiler survey, and the small slope failures or the marks of the debris flow are hidden by tresses.

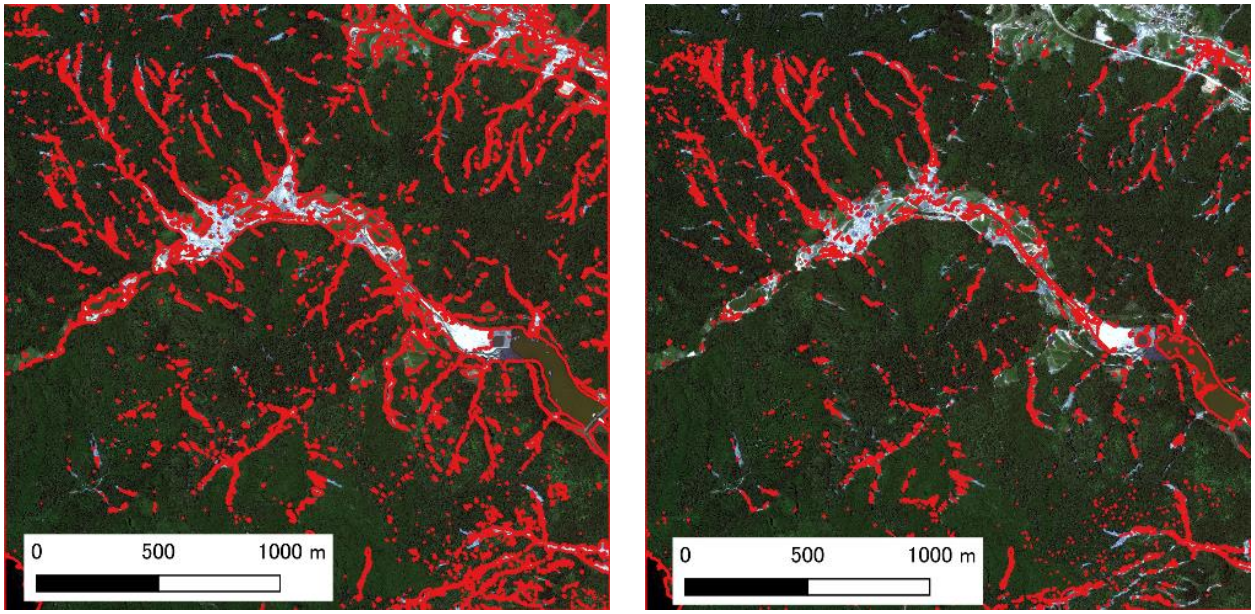

(a) Case B (b) Case C

Figure 3. Extraction results with NDVI and GSI

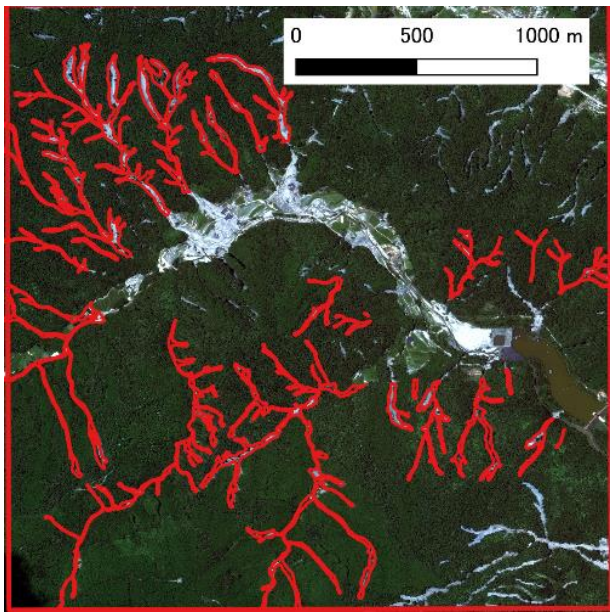

Figure 4. Slope failure obtained with Laser Profiler

3. RISK ANALYSIS FOR SEDIEMNT TO REACH RIVER

To evaluate the catchment area of the upstream side of Norogawa dam and the slope angles in the catchment area we used the DEM data provided by Geospatial Information Authority of Japan. The resolution of the DEM data is 5m.

According to the similar way of the risk management method proposed by Yano (2016), we have extracted the mountain streams which provide the sediments to the Norogawa River with the DEM data and GIS. The polygon surrounding the watershed was created in the GIS. Figure 5 shows the catchment area in the upstream side of Norogawa dam and the slope failures. The red line indicates the water shed. The inside of the closed area with the red line is the catchment area and the analytical target area. The region of the steep slope of which the slope angle is more than 30 degree was created. Figure 6 shows the distribution of the slope angle. The pink polygon indicates the slope angle which is more than and equal to 30 degree and less than 40 degree. The yellow polygon indicates the slope angle which is more than and equal to 40 degree. The slope failure occurrence points were estimated with GIS, and then the predicted reaching paths from the slope failure occurrence points to the Norogawa River were extracted by using the least-cost path analysis. In the least-cost path used here, the mountain stream on which the cost of the transportation from the slope failure occurrence point to the river was most minimized was chosen.

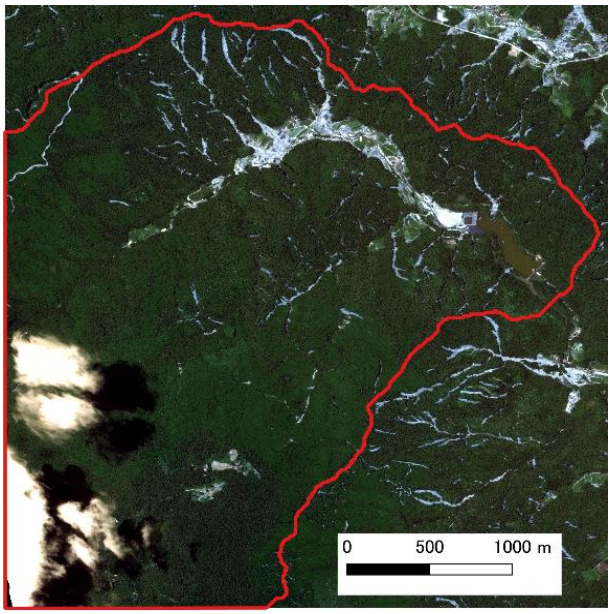

Figure 5. Catchment area and slope failure

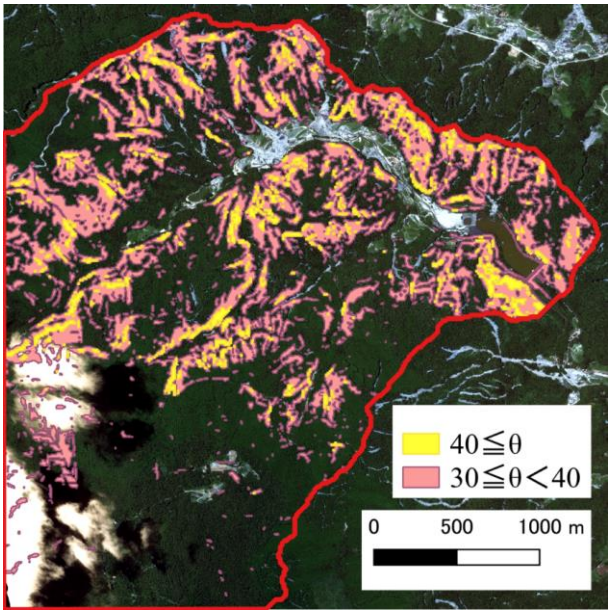

Figure 6. Distribution of slope angle

A maximum reaching path of sediment L_{max} is schematically shown in Figure 7. In this figure, θ is the slope angle, H is the height between the slope edge and the ground level, L is the horizontal distance from the slope failure occurrence point to the river, H' is the height between the slope failure occurrence point and the slope failure end point, L' is the horizontal distance from the slope failure occurrence point to the slope failure end point. If L_{max} is longer than L, the sediment can reach the river, so that we tried to choose the mountain stream along which the sediment can reach the Norogawa River using Eq. (3) proposed by Moriwaki (1987). Here after, we call this mountain stream a path reaching the river. On the other hand, the mountain stream along

which the sediment cannot reach the Norogawa River is called a path not reaching the river. The slope angel can be the important parameter in this analysis, so we conducted the investigations for three cases which are more than 30 degree, more than 40 degree and 50 degree.

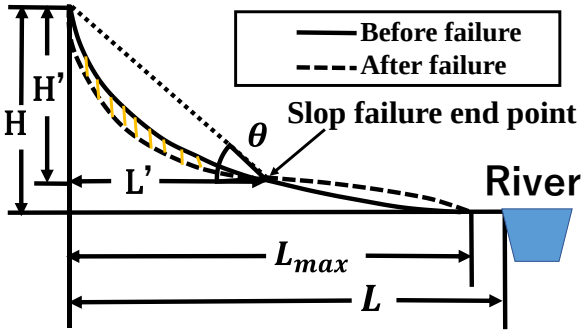

Figure 7. Schematic sketch of slope failure and maximum reaching path of sediment

$$\frac{L}{L_{\max}} = 0.73\tan\theta - 0.21 = 0.73\frac{H'}{L'} - 0.21 \tag{3}$$

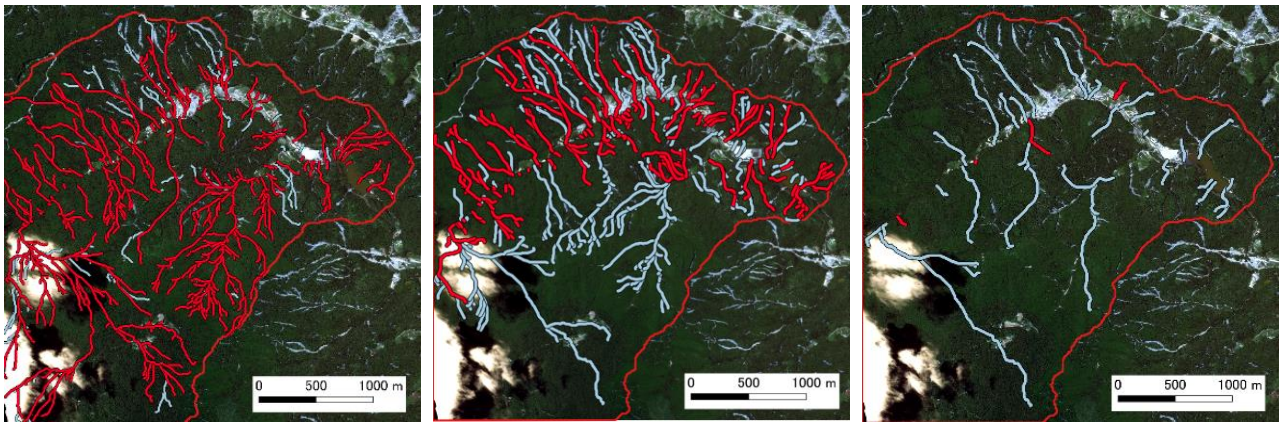

(a) 30 degree and greater (b) 40 degree and greater (c) 50 degree and greater

Figure 8. Path reaching (red line) and not reaching (blue line) river

Table 2. Number of paths reaching and not reaching river

	Slope angle		
	30 degree or greater	40 degree or greater	50 degree or greater
Path reaching river	425	260	4
Path not reaching river	98	245	37
Total number	523	405	41

Figure 8 shows the paths reaching the river and the paths not reaching the river. The red line indicates the path reaching the river, while the blue line indicates the paths not reaching the river. Table 2 shows the number of the path reaching the river and the path not reaching the river. For the case of 30 degree or greater 81.2% of all mountain streams in the analytical area were judged as the path reaching the river. As can be seen from Table 2, the total number of the mountain stream is 523. It is most number among the three cases. Generally, the mountain slope become steep as the grand level become high, so the slope failure end points of the high degree, such as 50 degree, are located on the high grand level. On the other hand, the slope failure end points of the low degree are located on the low grand level. So, the case of 30 degree or greater includes many mountain streams in the analytical area. Moreover, the distance to the river is relatively close to the river.

For the case of 40 degree or greater, the number of the path reaching the river and the path not reaching the river is comparable. For the case of 50 degree or greater, the number of the mountain stream is 41. This number is very much less than the case which is more than 30 degree. In addition, 90% of the mountain stream is the path not reaching the river in this case.

The difference number of the path reaching the river between the slope angles more than 30 degree and more than 40 degree is 165, and that between the slope angles more than 40 degree and more than 50 degree is 256. In the other words, there are 165, the path reaching the river in the slope angle between 30 and 40 degrees and are 256, the path reaching the river in the slope angle between 40 and 50 degrees. There are more risky mountain streams in the slope angle between 40 degree and 50 degree.

We have tried to confirm this risk analysis to the heavy rain disaster occurred July 2018. Table 3 shows the consistency number of the path reaching the river estimated by GIS to that detected with the optical satellite images. Similarly, table 4 shows the consistency number of the path not reaching the river estimated by GIS to that detected with the optical satellite images. In Table 3 Consistency means the number of the mountain stream that the same roots obtained with the optical satellite image and GIS are both the path reaching the river estimated. While "inconsistency" means the number of the stream that the path detected with the optical satellite image is the path reaching the river, but the same root estimated with GIS is not the path reach the river. The terms of "Consistency" and "Inconsistency" in Table 4 have the same meninges as Table 3, but these terms are used for the path not reaching the river.

Table 3. Consistency of number of paths reaching river estimated by GIS and optical satellite image

	Slope angle		
	30 degree or greater	40 degree or greater	50 degree or greater
Consistency	39 (68%)	41 (77%)	1 (5%)
Inconsistency	18 (32%)	12 (23%)	18 (95%)
Total number	57	53	19

For the case of 30 degree or greater in Table 3, the number of the path reaching the river detected with the optical satellite image is 57. Consistency is 39 and Inconsistency is 18. This risk analysis can estimate the mountain streams which have the risk to be the path reaching the river with 68% accuracy. On the other hand, although there are mountain streams estimated to be the path not reaching the river these mountain streams are the path reaching the river. It is 32% error. For the case of 40 degree or greater, the number of the path reaching the river is 53. Consistency and Inconsistency are 41 and 12, respectively. The proportions are 77% and 23%, respectively. For the case of 50 degree or greater, the number of the path reaching the river is 19. Consistency and Inconsistency are 1 and 18, respectively. The proportions are 5% and 95%, respectively. The proportion of Inconsistency increase as the slope angle increases. Comparing Table 2, we can see there are so many the path reaching the river for the slope angles range from 30 degree to 50 degree, but there are only 4 the path reaching the river for the slope angle range more than 50. Basically, there are not so much the estimated path reaching the river. However, 19 mountain streams were broken, and the sediment reached the Norogawa River actually.

Table 4. Consistency of number of paths not reaching river estimated by GIS and optical satellite image

	Slope angle		
	30 degree or greater	40 degree or greater	50 degree or greater
Consistency	10 (45%)	18 (64%)	13 (100%)
Inconsistency	12 (55%)	10 (36%)	0 (0%)
Total number	22	28	13

On the other hand, Table 4 shows the accuracy of the path not reaching the river. For the case of 30 degree or greater in Table 4, the number of the path not reaching the river detected the optical satellite image is 22. Consistency and Inconsistency are 10 and 12, respectively. The proportions are 45% and 55%, respectively. For the case of 40 degree or greater, the number of the path not reaching the river detected the optical satellite image is 28. Consistency and Inconsistency are 18 and 10, respectively. The proportions are 64% and 36%, respectively. For the case of 50 degree or greater, the number of the path not reaching the river detected the optical satellite image is 13. Consistency and Inconsistency are 13 and 0, respectively. The proportions are 100% and 0%, respectively. Contrary for Table 3, the accuracy of Consistency increase as the slope angle increase.

The real debris flows are able to join together and flow into the river. However, the least-cost path analysis does not include such physical process. It may cause inconsistency for path reaching river and path not reaching river.

4. CONCLUDING REMARKS

In this study, we have extracted the slope failures in the upstream region of Norogawa dam with the optical satellite images before and after the disaster occurred July 2018. In addition, by using the least-cost path analysis with GIS we have estimated the mountain stream along which the sediment produced by the slope failure can reach the Norogawa River or not.

NDVI and GSI images obtained from the optical satellite images before and after the disaster can reduce the extraction of the wrong bear fields, and the extraction accuracy of the slope failures is improved. It would be also anticipated that the extraction accuracy could be improved by processing the obtained image, furthermore, in terms of the slope angle or the position of the mountain stream.

For the least-cost path analysis, we have predicted the slope failure occurring point from the DEM data using GIS, and then have conducted the least-cost path analysis to extract the path reaching or not reaching the Norogawa River. The accuracy of this method was evaluated by comparing the slope failures occurred by the heavy rain disaster on July 2018. As a result, the prediction accuracy is the best if the slope angle is set to be 40 degree or greater. The accuracy of consistency for the path reaching the river is 77% and for the path not reaching the river is 64%. Of course, the mountain streams failed with the slope angle less than 40 degree are unable to be estimated if the slope angle is set to be 40 degree or greater. The improvement for this method is required. However, this risk analysis would be useful for the qualitative usage.

ACKNOWLEDGMENTS

This research was supported by Grant-Aid for Special Purposes, MEXT (18K19951). The Leaser Profile data was offered from the Sediment Control Division of Hiroshima Prefectural Office. We would like to express our appreciation for them.

REFERENCES

Eguchi, T. and Miura, F. (2016). Study on the method to detect slope failure areas due to earthquakes and heavy rains by using satellite remote sensing, Journal of JSCE F6, Vol.72, No1, pp.11-20. (In Japanese).

Hayashi, H., Mizuno, M., Osanai, N., Nishi, M., Shimizu, Y., Nakagawa, K. and Matsumoto, S. (2012). Applicability of methods for detecting landslides by using synthetic aperture radar of ALOS(Daichi), *Journal of Erosion Control Engineering*, Vol.65, No.4, pp.3-14, (In Japanese).

Moriwaki H. (1987). A Prediction of the Runout Distance of a Debris, *Journal of Japan Landslide Society*, Vol.24, No.2, pp.10-16, (In Japanese).

Yano, S., Tsuchihashi, S., Dozono, S., Kazama, K. and Kita, T. (2016). Assessment of woody debris disaster risk at all bridges along the Kagetsu river according to its generation potential concept, Journal of JSCE B1, Vol.72, No.4, pp. I_289-I_264. (In Japanese).